

Low-energy lattice vibrations of porous silica glass

Susan K. Watson* and R. O. Pohl

Laboratory of Atomic and Solid State Physics, Cornell University, Ithaca, New York 14853, USA

(Received 12 August 2002; revised manuscript received 3 March 2003; published 23 September 2003)

Internal friction, speed of sound, and thermal conductivity of Vycor glass with porosities ranging from 29% to 36% have been measured from 65 mK to 300 K. The results have been compared with those obtained on bulk amorphous silica in order to understand how the porous structure affects the low-energy tunneling states. Contrary to specific-heat results reported previously on Vycor, our measurements indicate that these changes are surprisingly small. Our findings agree qualitatively with the results reported previously on sol-gel porous glass with a similar porosity, and also on aerogels, which are even more highly porous than Vycor. Analysis of the porous silica data suggests that the porosity has very little influence on the spectral density of the tunneling defects, while their coupling energy to the phonons scales with the speed of sound. The excitations observed in specific heat, however, appear to be different from those observed in the acoustic and thermal-conductivity experiments.

DOI: 10.1103/PhysRevB.68.104203

PACS number(s): 62.40.+i, 63.20.-e, 63.50.+x

I. INTRODUCTION

The low-energy lattice vibrations of amorphous solids are dominated by tunneling states, also known as two-level systems (TLS), which are responsible for their thermal, acoustic, and dielectric properties. The phenomenological Tunneling Model, proposed by Anderson, Halperin, Varma¹ and independently by Phillips² in 1972 to describe the thermal properties of amorphous solids, and extended by Jäckle³ to describe the acoustic properties, has generally been highly successful. Based upon a few plausible assumptions, the Tunneling Model is able to account for an impressive array of low-temperature properties.⁴⁻⁶ It should be noted, however, that the model makes no attempt to explain the microscopic nature of the tunneling entities nor their nearly universal spectral density of states, \bar{P} , which was found through numerous studies to be surprisingly insensitive to the chemical bonding or physical properties of amorphous solids.⁷

Much effort has been directed towards uncovering the cause of this universal spectral density. The most promising ideas involve the role of interactions between TLS, which had been ignored in the Tunneling Model. Soon after it was reported that amorphous solids appear to have very similar anomalous thermal properties at low temperatures,⁸ Klein *et al.*⁹ speculated that strain-mediated interactions between the tunneling entities could be responsible for this similarity. By comparing many amorphous solids, Freeman and Anderson¹⁰ found that the tunneling strength $C = \bar{P} \gamma^2 / \rho v^2$ rather than the spectral density \bar{P} was the quantity that varied least between amorphous solids (γ —coupling of TLS to phonons; ρ —mass density; v —speed of sound), as had been noted previously by Hunklinger *et al.*¹¹ Freeman and Anderson argued that the universality of this combination of parameters was an indication of the role of strain-mediated interactions between TLS.

Theoretical work by several researchers has addressed the effects of interactions,¹²⁻¹⁹ but to date none of these theories appear to have been unambiguously confirmed by experiment. The reason for this is in part that the experimental

evidence for interactions between TLS is contradictory. Pulse-echo experiments on borosilicate glass indicated the existence of elastic interactions between neighboring TLS.^{5,20} Dielectric measurements on silicate glasses and Mylar^{21,22} were found to be consistent with the predictions of interacting TLS models.^{16,18,23} Several measurements could not be explained within the context of the present noninteracting TLS theory, including internal friction and sound speed measurements²⁴ of Zr_xCu_{1-x} and sound speed measurements²⁵ of *a*-SiO₂ thin films of thickness 20–500 nm. However, internal friction measurements²⁶ of atomically flat *a*-SiO₂ films ranging in thickness from 0.75 nm to 1000 nm showed no deviation from bulk *a*-SiO₂ values below 1 K, although one would expect that the finite size of the films should affect interactions on length scales longer than the film thickness, thereby increasing the spectral density of TLS.

The first study of the lattice vibrations of finely subdivided amorphous solids was performed by Stephens²⁷ who measured the thermal conductivity below 1.5 K of Vycor glass, a silica glass with interconnected pores of ≈ 7 –8 nm diameter and a porosity of 29% (further details on this porous glass can be found in Sec. II). He found its thermal conductivity to approach that of bulk *a*-SiO₂ at the lowest temperatures. Since these measurements will be used later in the discussion of our results, they are reproduced here in Fig. 1 (labeled “Vycor29”; note that all porous samples discussed in this study are labeled according to their porosity; see Table I). The influence of the porosity was subsequently studied by Tait²⁸ by extending the thermal-conductivity measurements to 30 K, also shown in Fig. 1. The two datasets do not agree completely in the temperature region of overlap; in the following, both datasets will be analyzed. The top axis of the figure indicates the dominant phonon wavelength, λ_{dom} for Vycor29, i.e., the wavelength corresponding to the phonons which transport the majority of the heat.²⁹ At $T = 1$ K, the dominant phonon wavelength for Vycor29 is $\lambda_{dom} = 27$ nm as compared to an average pore diameter of 7.5 nm and an average pore separation of ≈ 9.0 nm or 12.5 nm, estimated assuming either spherical or cylindrical pores, respectively.

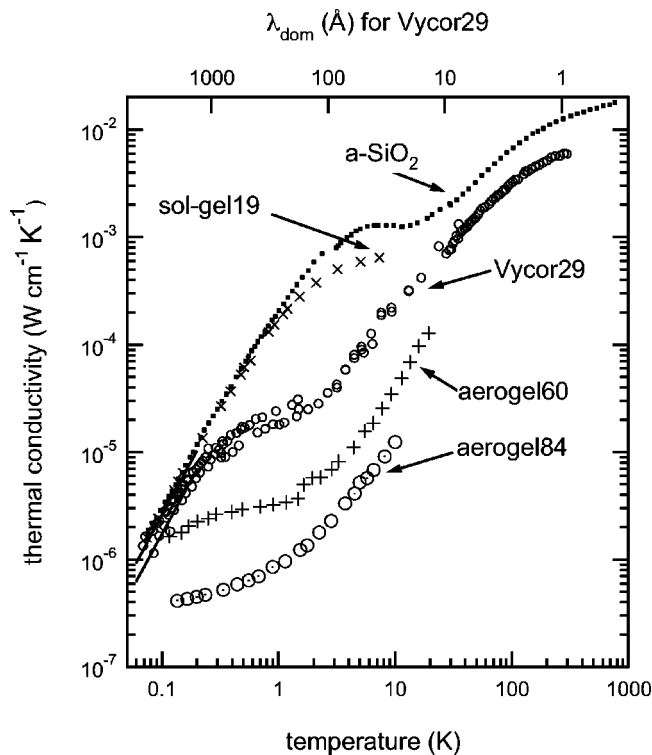


FIG. 1. Thermal conductivity of bulk $a\text{-SiO}_2$ compared to several porous silica samples described in the text ($a\text{-SiO}_2$, Ref. 66; sol-gel19, Ref. 30; Vycor29: Ref. 27 below 1.5 K, Ref. 28 below 30 K, and this work $10\text{ K} \leq T \leq 300\text{ K}$; aerogel60, Ref. 34; aerogel84, Ref. 34; see Table I). Although the thermal conductivities of the materials differ significantly at intermediate temperatures where scattering by voids dominates, the thermal conductivities of all porous samples approach that of bulk $a\text{-SiO}_2$ at the lowest temperatures where phonons are believed to be scattered mainly by TLS. The solid lines in the figure indicate T^2 fits to the Vycor29 data.

For comparison, the dominant phonon wavelength for aerogel84 is estimated to be 5.9 nm at $T=1\text{ K}$.

The suppression of the thermal conductivity of Vycor compared to bulk $a\text{-SiO}_2$ above $T \sim 300\text{ mK}$ has been explained by Grace and Anderson³⁰ through phonon scattering by the voids. The lowering of the thermal conductivity by a constant factor (2.1) relative to that of the bulk glass above 30 K can be explained by an effective reduction of the cross section through which the heat diffuses, as reviewed in Ref. 31. For the present discussion, only the data below 1 K need concern us. At these temperatures the thermal conductivity of Vycor may be interpreted as evidence for the presence of tunneling states which are quantitatively very similar to those in bulk $a\text{-SiO}_2$. By contrast, the low-temperature specific heat showed a significant enhancement over that observed in the bulk glass, as shown in Fig. 2 (see also Ref. 28, as reviewed in Ref. 32).³³ Measurements by Grace and Anderson³⁰ on another porous glass produced by the sol-gel process, which had smaller pore sizes ($\sim 2\text{ nm}$ in diameter; porosity 19%), yielded similar results: A thermal conductivity identical to that of bulk $a\text{-SiO}_2$ up to $\sim 1\text{ K}$, as shown in Fig. 1, and a linear specific heat even larger than that of Vycor, see Fig. 2.

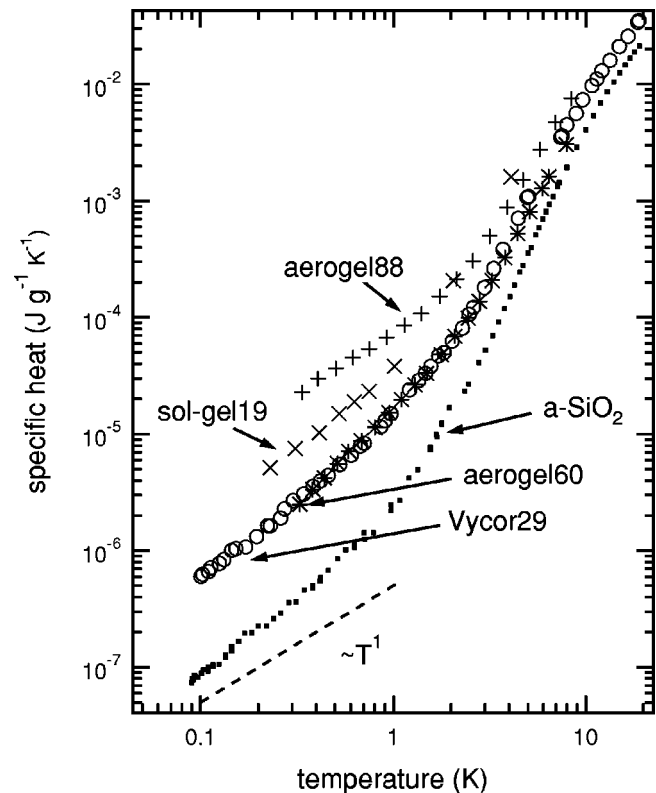


FIG. 2. Specific heat of bulk $a\text{-SiO}_2$ compared to several porous silica samples described in the text (aerogel88, Ref. 34; sol-gel19, Ref. 30; aerogel60, Ref. 34; Vycor29, Ref. 28). In contrast to the thermal conductivity, the specific heat below 1 K for the porous silica samples is significantly enhanced relative to bulk $a\text{-SiO}_2$. The dashed line labeled T^1 indicates the linear temperature dependence predicted by the Tunneling Model. (Fits to the low-temperature data of the form $C=A_0T^1$ yield $A_0=9.7 \times 10^{-7}$ for $a\text{-SiO}_2$; $A_0=5.8 \times 10^{-6}$ for Vycor29 and aerogel60; $A_0=2.3 \times 10^{-5}$ for sol-gel19; and $A_0=7.3 \times 10^{-5}$ for aerogel88 in units $\text{J g}^{-1} \text{K}^{-1}$. In order to convert the published aerogel data, we used $1.0\text{ J g}^{-1} \text{K}^{-1} = 60.09\text{ J mole}^{-1} \text{K}^{-1}$.)

Qualitatively similar results were observed on yet another kind of porous silica, aerogels, which were studied by de Goer *et al.*³⁴ and by Bernasconi *et al.*³⁵ These glasses consist of filaments $\approx 4\text{ nm}$ in diameter; the mass densities of the aerogels studied ranged from 0.87 to 0.12 g cm^{-3} corresponding to porosities ranging from 60% to 95%. While the thermal conductivity³⁴ of the sample with the lowest porosity (aerogel60, $\rho=0.87\text{ g cm}^{-3}$; Fig. 1) appears to approach that of bulk $a\text{-SiO}_2$ at the lowest temperatures, its specific heat³⁴ is close to that of Vycor29 (Fig. 2). For a higher porosity aerogel (aerogel84, $\rho=0.36\text{ g cm}^{-3}$; Fig. 1), the measuring temperature was not low enough to tell whether the thermal conductivity approaches that of bulk $a\text{-SiO}_2$; the specific heat³⁴ of a sample with similar porosity (aerogel88, $\rho=0.27\text{ g cm}^{-3}$; Fig. 2) is distinctly higher even than that of sol-gel19. Amazingly, a further reduction of the mass density had only very little influence on the specific heat, which stayed close to that of the sample with the 0.27 g cm^{-3} mass density, even as the latter decreased to 0.12 g cm^{-3} (Ref. 34) and 0.145 g cm^{-3} (Ref. 35; data not shown in Fig. 2). De

TABLE I. Properties of bulk a -SiO₂ and several porous materials, including the Vycor samples measured in this work. The names of the porous materials correspond to their porosities, with the sample porosity determined from the relation $p=1-\rho/\rho_o$, where ρ_o is the mass density of bulk a -SiO₂. [Note that in previously published work on the aerogels, aerogel60 was named “Sample a (Ref. 68) or BC 0.87 (Ref. 34); aerogel80 was named A-NC 0.36 (Ref. 34); and aerogel88 was named Sample c (Ref. 68) or BC 0.27 (Ref. 34).]

Material	Average pore diameter (Å)	Density ρ (g cm ⁻³)	Porosity p	Transverse sound velocity v_t (10 ⁵ cm s ⁻¹)	Longitudinal sound velocity v_l (10 ⁵ cm s ⁻¹)
a -SiO ₂ ^a		2.20	0	3.8	5.8
Vycor4 ^b		2.115	0.04	3.55	
Sol-gel19 ^c	20	1.79	0.19	1.8	3.1
Vycor29 ^d	75	1.57	0.29	2.14	
Vycor29 ^e		1.558	0.29	2.19	
Vycor35 ^f	20	1.44	0.35	2.06	
Vycor36 ^f	36	1.42	0.36	2.04	
Aerogel60 ^g		0.87	0.60		1.85
Aerogel84 ^g		0.36	0.84		0.78
Aerogel88 ^g		0.27	0.88		0.425

^aReference 7. Note also that in Ref. 69, Table 1, nearly identical values are listed for three different bulk a -SiO₂ samples including Suprasil W, i.e., bulk a -SiO₂ with low OH content, which is used for comparison to the porous a -SiO₂ materials throughout this work.

^bReference 41. According to the authors, the sample was created by fusing Vycor29 in order to eliminate the pores.

^cReference 30. Sound velocities were measured at room temperature at 13 MHz using a pulse-echo technique. The same values were determined at 2×10^{10} Hz from Brillouin scattering.

^dMaterial used in present study: Corning Code 7930. The pore diameter and density were determined by Tait (Ref. 37), who found a pore diameter between 7.0 and 8.0 nm; the average of those values is listed here. The transverse speed of sound is measured in the present work.

^eReference 41. The transverse sound velocity was measured at $f=20$ MHz using a pulse-echo technique.

^fValues for the average pore diameter and total pore volume per unit mass (cm³ g⁻¹) were supplied by Elmer (Ref. 44). Transverse sound velocities are estimates based upon an empirical relation between porosity and elastic modulus which has been found to hold for several porous materials [see Eq. (1)] (Ref. 48).

^gReference 34; Speeds of sound were measured at $f=10$ MHz at room temperature.

Goer *et al.*³⁶ also measured the low-temperature internal friction of samples ranging from 0.27 to 0.87 g cm⁻³. They found a nearly temperature-independent plateau below ~ 5 K, of a magnitude close to that of bulk a -SiO₂. These data will be shown below together with our measurements of Vycor.

The measurements on porous glasses which have been reviewed here can be summarized by the statements that their thermal conductivities appear to approach that of bulk a -SiO₂ at sufficiently low temperatures, while the specific-heat anomaly greatly exceeds that of the bulk glass. An interpretation of both observations in terms of the Tunneling Model would require that the energy-independent spectral density \bar{P} of the tunneling states increases with increasing porosity (reaching a saturation at the very largest porosities), in order to explain the increase of the specific heat, while their coupling strength to the phonons decreases so as to keep the thermal-conductivity constant. The Cornell authors^{27,28,32,37} were skeptical of such an interpretation and suggested instead that one should consider the possible role of localized excitations either of surface atoms or of adsorbed gases. Their vibrational excitations would be seen in

specific heat but might not couple strongly to the phonons. A different explanation of these observations on the aerogels was given by de Goer *et al.*³⁴ and by Bernasconi *et al.*³⁵ who argued that although TLS are present within the silica filaments with properties very similar to TLS in bulk a -SiO₂, a consistent interpretation of all of the measurements on aerogels could be found in their fractal structure (see also Ref. 38). After repeating the measurements of the specific heat of Vycor, and after also studying its low-temperature heat release, Nittke, Esquinazi, and Burin³⁹ concluded that the states seen in the measurements are indeed tunneling states as seen in bulk amorphous solids. However, by finely subdividing the solid, elastic interactions between those states are hindered at low temperatures, and consequently more tunneling states can remain active. This interpretation was based on the assumption that in bulk glasses the tunneling states are frozen-in at low temperatures due to strain-mediated interactions, and they took their measurements as proof of this assumption. In order to explain the unchanged thermal conductivity in the Vycor, their interpretation required that the free (i.e., not frozen-in) tunneling states would scatter the thermal phonons less, which the authors considered to be possible. In

a more recent work by Nittke *et al.*,⁴⁰ the specific heat and heat release of micron-sized α -SiO₂ particles were interpreted in a similar manner.

The same study⁴⁰ illustrated the difficulty of interpreting specific-heat results for porous or highly compacted materials. The authors found that the specific heat of micron-sized α -SiO₂ particles embedded in teflon was significantly enhanced relative to bulk α -SiO₂ after subtracting the contribution of the teflon. However, they also found that the specific heat of quartz particles embedded in teflon was larger than bulk α -SiO₂ (i.e., significantly larger than the specific heat of quartz), despite the fact that x-ray-diffraction patterns of the quartz particle samples revealed crystalline structure. Early work by Tait on compacted crystalline alumina particle samples and on compacted 7 nm diameter α -SiO₂ particle samples likewise revealed that specific-heat measurements on porous and compacted materials are very confusing (see Ref. 28 as reviewed in Ref. 32).

Nittke *et al.* ascribed the enhanced specific heat of their quartz particle samples to surface defects. The Vycor, sol-gel, and aerogel materials considered in Fig. 2 have very large internal surface areas, making surface defects a possible explanation for the enhanced specific heat in those materials as well. Given the consistency of specific-heat results between various research groups and the precautions taken to avoid adsorbed gases, it is unlikely that these states, if they exist, are surface contaminants. They are more likely intrinsic surface molecules or groups of molecules with somewhat different chemical bonding than in the bulk.

In light of the discrepancies and unanswered questions regarding the porous silicas, it appeared desirable to add low-frequency acoustic measurements of Vycor to those of thermal conductivity and specific heat; to explore how a variation of the porosity of Vycor affects the thermal conductivity; and, through a comparison with existing high-frequency acoustic data on Vycor,⁴¹ to explore whether the tunneling strength is independent of frequency for porous materials, as has been found to be the case for bulk amorphous solids.⁵ These measurements will be presented here and will be analyzed together with those on the thermal conductivity reported previously. It will be seen that all observations—except those of the specific heat—can be described consistently with the Tunneling Model, with a tunneling strength C which is independent of the elastic moduli of the glasses over a range of three orders of magnitude. The excitations observed in specific heat appear to have a different origin from those observed in the acoustic and thermal-conductivity experiments.

II. EXPERIMENTAL MATTERS

Vycor is produced by dissolving the boron-rich phase out of a phase-separated borosilicate glass, leaving behind a porous silica network composed of 96% α -SiO₂.^{37,42,43} The Vycor with the largest pore diameter (Vycor29, Corning code 7930) was previously measured and characterized by Tait^{28,37} who performed gas adsorption experiments to determine a mass density for Vycor29 of 72% the value of bulk α -SiO₂ and an average pore diameter of 7–8 nm. The remaining

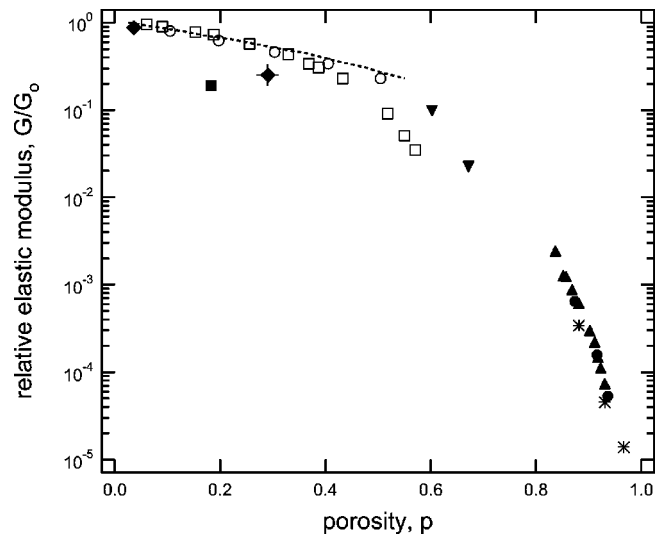


FIG. 3. Relative elastic modulus as a function of porosity for porous silica aerogels, sol-gel, and Vycor (solid symbols) and for porous Greenland snow and alumina (open symbols), after Hessinger *et al.*, Ref. 48. For the silica aerogels, Vycor, and Greenland snow the data were extracted from measurements of the shear modulus $G_{porous}/G_{nonporous}$; for porous alumina, the Young's modulus was used. The dashed line is a theoretical curve from MacKenzie (Ref. 46) and Kingery *et al.* (Ref. 47). [Silica aerogels: *, Ref. 49; ●, Ref. 50; ▲, Ref. 51; ▼, Ref. 52. Sol-gel: ■, Ref. 30. Vycor: ◆, Ref. 41; +, this work (the two data points for Vycor29 overlap). Greenland snow: □, Ref. 53. Porous alumina: ○, Ref. 54.]

Vycor samples were supplied to us by Maris who obtained them from Elmer of the Corning Research Laboratory.⁴⁴ Due to the extremely large internal surface area of Vycor (~ 89 m²/g for Vycor29),²⁸ care was taken in cleaning the samples in order to minimize the effects of adsorbed molecules. Details on the cleaning procedure and fabrication technique can be found in Ref. 45.

Table I summarizes the properties of the Vycor samples used in this study as well as several additional porous α -SiO₂ materials measured elsewhere and discussed here. The data are compared to Suprasil W (i.e., bulk α -SiO₂ with a low OH content); the properties of bulk α -SiO₂ are therefore listed in the table as well. The transverse sound velocity of Vycor29 was determined in this study (see Sec. IV). For the Vycor samples with 2.0 nm diameter pores (Vycor35) and 3.6 nm diameter pores (Vycor36), the samples were too small to perform sound speed measurements with our setup. Therefore, the sound speeds listed for those materials were estimated from an empirical relation^{46,47} between porosity and elastic modulus which has been found to hold for porous materials including Vycor, aerogel, alumina, and Greenland snow with porosities less than 0.5 (dashed line in Fig. 3):

$$G = G_o(1 - 1.9p + 0.9p^2). \quad (1)$$

Here p refers to the sample porosity; for the elastic modulus $G_o = \rho_o v_t^2$ we use the values listed in Table I for Vycor29 (i.e., since the relative elastic modulus for Vycor29 falls below the empirical relation indicated by the dashed line in Fig.

3, the transverse speeds of sound for Vycor35 and Vycor36 have been scaled to the value for Vycor29).

Thermal-conductivity measurements above 30 K were performed using an ac technique for which errors due to blackbody radiation are negligible.⁵⁵ For measurements below 30 K a standard dc technique was used with two thermometers and one heater (see Ref. 56 for more details). For the dc measurements, heaters and thermometers were pressed against samples with indium-coated BeCu clamps rather than attached with glue since glue may penetrate into porous samples. The Vycor samples used for dc measurements were small and somewhat irregular in shape due to multiple nicks along their edges (Vycor35: area = 0.18×0.16 cm²; distance between thermometers = 0.74 cm; Vycor36: area = 0.15×0.20 cm²; distance between thermometers = 1.16 cm for measurements below 1 K and 0.60 cm for measurements above 1 K). For the Vycor35 dc measurements, identical thermometer clamp positions were used for data above and below 1 K. For the Vycor36 dc measurements, different thermometer clamp positions were required for data above and below 1 K since one end of the sample broke after the $T \leq 1$ K run. The geometrical scaling factor (sample area divided by thermometer separation) was therefore less certain for the Vycor36 sample in the intermediate temperature range. The data have been adjusted by a constant factor of 0.75 to match smoothly with the ac data above 30 K (no adjustments were made to the $T \leq 1$ K or $T \geq 30$ K data).

The internal friction and speed of sound of Vycor29 were measured in torsion using a compound oscillator technique that ensures good thermal contact between sample and cryostat.⁵⁷⁻⁵⁹ Samples were epoxied to a quartz transducer, the opposite end of which was attached to a thin BeCu pedestal (for each joint, $a \sim 0.5$ -mg drop of Stycast 2850FT epoxy was used). Dimensions for the Vycor29 sample (area = 0.15×0.15 cm²; length = 1.33 cm) were chosen to create a stress node at the quartz-sample interface in order to minimize mounting losses. The background loss due to the mounting arrangement was negligible below 10 K ($< 4 \times 10^{-6}$) and has not been subtracted from the data. The small sizes of the Vycor35 and Vycor36 samples precluded their use in internal friction measurements.

In an experiment, the internal friction of the compound oscillator consisting of sample and transducer, Q_{co}^{-1} , is directly measured; the internal friction of the sample, Q_s^{-1} , can be determined from

$$Q_s^{-1} = \left[(1 + \alpha) \frac{I_t}{I_s} + 1 \right] Q_{co}^{-1}, \quad (2)$$

where I_t and I_s are the moments of inertia of the transducer and sample, respectively, relative to the torsion axis along the length of the composite oscillator, and α is an empirical factor used to account for the finite thickness of the BeCu pedestal ($\alpha \sim 0.06$).^{59,60} The change in transverse sound velocity of Vycor29 was simultaneously measured by monitoring the shift in resonant frequency of the compound oscillator.⁶⁰

$$\left(\frac{\delta v}{v_o} \right)_s = \left[(1 + \alpha) \frac{I_t}{I_s} + 1 \right] \left(\frac{\delta f}{f_o} \right)_{co}. \quad (3)$$

(The resonant frequency of the compound oscillator with Vycor29 mounted was 88.3 kHz at room temperature, a 2% shift from the 90 kHz resonant frequency of the quartz transducer with no sample mounted.) The transverse sound velocity determined from the resonant frequency of the compound oscillator was found to be $v_t = 2.14 \times 10^5$ cm/s at 78 K, in close agreement with the value $v_t = 2.19 \times 10^5$ cm/s determined from ultrasonic measurements⁶¹ at $f \sim 10$ MHz on the same material at 77 K. For internal friction and speed of sound measurements, care was taken to avoid self-heating of the sample below 100 mK by maintaining the drive amplitude at a low enough value to stay well within a linear-response regime.

For all measurements, precautions were taken to minimize the effects of adsorbed gases in the interiors of the samples. For thermal-conductivity measurements below 1 K, ⁴He exchange gas was used in the vacuum can from room temperature to 30 K, at which point the sample space was evacuated to less than 10^{-6} torr. For thermal-conductivity measurements above 1 K and for internal friction measurements, the sample space was evacuated to less than 10^{-6} torr at room temperature; no exchange gas was subsequently used. Bernasconi *et al.*⁶² have shown that adsorbed H₂ or O₂ has a negligible effect on the thermal conductivity from 2 K to 20 K of aerogel samples with similar internal surface areas as the Vycor samples used in this study. For the present measurements, where significantly less ⁴He gas was adsorbed than either H₂ or O₂ in the study of Bernasconi *et al.*, it is safe to assume that the measured thermal conductivities are intrinsic.

III. TUNNELING MODEL AND DATA ANALYSIS

Theoretical predictions for the TLS effects on the thermal conductivity and internal friction are summarized here for later comparison to experimental results. From the Tunneling Model, the thermal conductivity of an amorphous solid below 1 K varies as T^2 due to phonon scattering from TLS:

$$\Lambda(T) = \frac{\rho k_B^3 T^2}{6 \pi \hbar^2 \bar{P}} \left(\sum_{\alpha} \frac{v_{\alpha}}{\gamma_{\alpha}^2} \right) \quad (4)$$

(ρ —mass density; v —sound velocity; γ —coupling of TLS to phonons; α —transverse or longitudinal phonon mode). The expression may be simplified using the following empirical relations⁷ which have been found to hold for many amorphous solids:

$$v_l \approx 1.65 v_t \quad \text{and} \quad \gamma_l^2 \approx 2.5 \gamma_t^2, \quad (5)$$

where the subscripts t and l refer to transverse and longitudinal phonon modes, respectively. In this work, the following expression is used to fit the data in order to extract the prefactor β_o and the value of the tunneling strength $C_t = \bar{P} \gamma_l^2 / \rho v_l^2$:

$$\Lambda(T) = \frac{2.66k_B^3}{6\pi\hbar^2} \frac{1}{C_t v_t} T^2 = \beta_o T^2. \quad (6)$$

The tunneling strength also may be determined from the internal friction, which is a measure of the energy lost per oscillation cycle relative to the mechanical energy stored per cycle. The Tunneling Model prediction for the internal friction takes on simple closed form expressions in two limiting cases of interest. In the extreme low-temperature limit, the maximum relaxation rate τ_{max}^{-1} of the TLS is small relative to the frequency of the applied strain oscillations, $\tau_{max}^{-1} \ll \omega$. As a result, the TLS are too slow to respond to the oscillating strain field, and their contribution to the internal friction drops as T^3 with decreasing temperature.⁶³ At higher temperatures, where the TLS relax quickly enough to reach equilibrium on the time scale of an oscillation, $\tau_{max}^{-1} \gg \omega$, the internal friction is constant:

$$Q^{-1} = \frac{\pi^4}{96} C_t \left[\frac{T}{T_{co}} \right]^3 \quad (T \ll T_{co}) \quad (7)$$

$$= \frac{\pi}{2} C_t \quad (T \gg T_{co}), \quad (8)$$

where C_t is the tunneling strength. T_{co} indicates the crossover temperature between the two limiting regimes, i.e., the temperature at which the maximum relaxation rate of the TLS is equal to the frequency at which the oscillator is driven:

$$T_{co} = \left[\frac{2\pi\rho\hbar^4\omega}{8k_B^3 \left(\frac{\gamma_t^2}{v_t^5} + 2\frac{\gamma_t^2}{v_t^5} \right)} \right]^{1/3}. \quad (9)$$

In order to extract the tunneling strength C_t , we fit the internal friction data to a constant value over the temperature-independent ‘‘plateau’’ region [Eq. (8)]. In addition, the transverse coupling between TLS and phonons, γ_t , can be calculated from T_{co} , which is extracted by fitting the data to a full numerical evaluation^{59,64} of the Tunneling Model prediction. In the fit, T_{co} is the only adjustable parameter along the temperature axis; Eqs. (5) are used to express T_{co} in terms of transverse quantities.

The presence of TLS also affects the variation of sound speed in amorphous solids, with Tunneling Model predictions given by

$$\frac{\delta v}{v_o} = \frac{v - v_o}{v_o} = C_t \ln \left(\frac{T}{T_o} \right) \quad (T \ll T_{co}) \quad (10)$$

$$\frac{\delta v}{v_o} = \frac{-C_t}{2} \ln \left(\frac{T}{T_o} \right) \quad (T \gg T_{co}). \quad (11)$$

Here v_o is the velocity at an arbitrary reference temperature T_o (not to be confused with the crossover temperature T_{co}). According to the Tunneling Model, the values for the tunneling strength C_t and the coupling constant γ_t extracted from internal friction and speed of sound data should be identical.

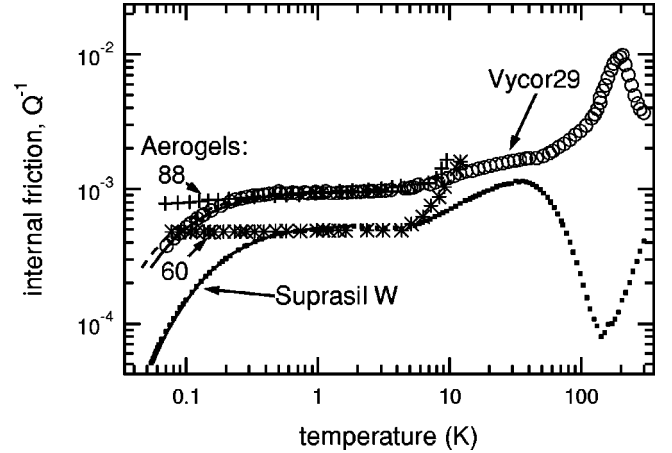


FIG. 4. Internal friction of Vycor29 (this work), Suprasil W (Refs. 57 and 64) and two high-porosity aerogel samples (Ref. 68). Both Vycor29 and Suprasil W were measured in torsion using a composite oscillator technique with an excitation frequency of ~ 66 kHz (Suprasil W) and ~ 88 kHz (Vycor29). The aerogel samples were measured in flexure at 3.4 kHz (aerogel60) and 1.0 kHz (aerogel88) (Ref. 68). In the plateau region where the internal friction scales directly with the tunneling strength $C = \bar{P}\gamma^2/\rho v^2$, the internal friction of Vycor29, aerogel, and Suprasil W differ by less than a factor of 2 despite significant differences in the structures of the materials. Solid lines indicate Tunneling Model fits to the data, with $T_{co} = 47$ mK for Vycor29 and $T_{co} = 84$ mK for Suprasil W. The dashed line through the Vycor29 data is a Tunneling Model fit using the value $T_{co} = 40$ mK derived from the speed of sound data, indicating the consistency of parameters derived from both types of measurements.

We note, however, that VanCleve *et al.*⁵⁹ and Classen *et al.*⁶⁵ have found that in many cases no single choice of parameters fits both $\delta v/v$ and Q^{-1} in all temperature regions equally well. In the following, we extract values for γ_t from both internal friction and speed of sound data, keeping in mind the preceding cautionary statement.

IV. RESULTS

The internal friction of porous Vycor29 is typical of amorphous solids, as illustrated in Fig. 4 by a comparison with bulk α -SiO₂ (labeled ‘‘Suprasil W’’). For both materials there are broad peaks above 10 K which have been explained through thermally activated processes. In this temperature region, the internal friction does not exhibit universal behavior and there is significant variation between amorphous solids.⁶⁶ Below ~ 10 K, where TLS are believed to dominate, both materials show the characteristic plateau region followed by a drop-off at the lowest temperatures where the maximum relaxation rate of the TLS becomes smaller than the frequency of the oscillating strain field.

The variation in sound speed for Vycor29 is also found to be consistent with the behavior expected for bulk amorphous solids (Fig. 5). Data below 1 K for Vycor29 and Suprasil W both exhibit a characteristic maximum at the crossover between the low-temperature data of positive slope [Eq. (10)] and the higher-temperature data of negative slope [Eq. (11)].

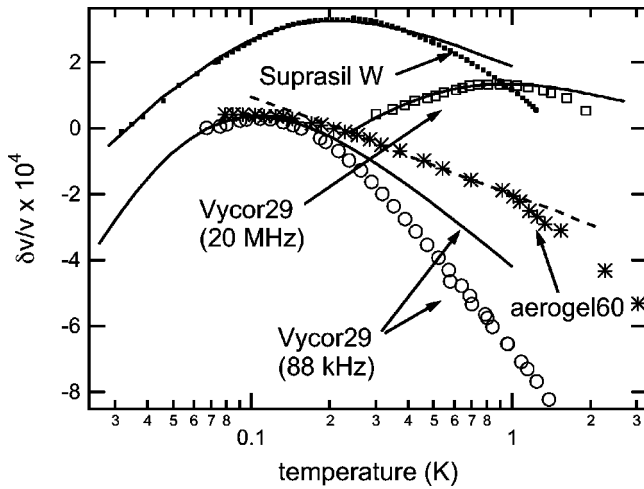


FIG. 5. Relative change in speed of sound for Vycor29 (this work; $f=88$ kHz) and Suprasil W (Ref. 67; $f=66$ kHz) measured in torsion; high porosity aerogel60 (Ref. 68; $f=3.4$ kHz) measured in flexure; and Vycor29 (Ref. 41; $f=20$ MHz) from transverse ultrasound measurements. The relative change in speed of sound for porous Vycor29 is qualitatively similar to bulk a -SiO₂, with both materials exhibiting a characteristic peak below 1 K. The data are well fit by the Tunneling Model (solid lines) in the temperature region below the peak where the best agreement is typically found between internal friction and variation in sound speed data. For the low-frequency data, the shift in peak position to lower temperature for Vycor29 compared to Suprasil W indicates the lower cross-over temperature T_{co} in Vycor29 ($T_{co}=40$ mK for Vycor29; $T_{co}=80$ mK for Suprasil W) due to its smaller mass density and sound velocity. Although the aerogel60 data do not reach a low enough temperature to reveal the possible existence of a peak, the logarithmic temperature dependence in the region $0.2 \leq T \leq 1$ K is characteristic of bulk amorphous solids [Tunneling Model fit to aerogel60 data (dashed line) is from Ref. 68].

The shift of the peak to lower temperature in Vycor29 (88 kHz data) compared to Suprasil W reflects the lower cross-over temperature T_{co} in Vycor29 due to its smaller mass density and sound velocity ($T_{co}=40$ mK for Vycor29 vs 80 mK for Suprasil W). Unfortunately, no data therefore exist below the peak which, however, is clearly indicated. Since the location of the peak scales with frequency [Eq. (9)], high-frequency 20-MHz data by Beamish *et al.*⁴¹ resolve the peak more clearly, and are shown in Fig. 5 for comparison. The transverse speed of sound for Vycor29 at 78 K, as determined from the resonant frequency of the composite oscillator, is found to be $v_t=2.14 \times 10^5$ cm/s (see Table I and Sec. II).

Tunneling Model fits to the internal friction and variation in sound speed data for Vycor29 and Suprasil W are shown by solid and dashed lines in Figs. 4 and 5. Best fits to the internal friction data yield $T_{co}=47$ mK for the Vycor29 data and $T_{co}=84$ mK for Suprasil W (note that T_{co} is the only free parameter along the temperature axis). Since no data exist below the maximum for the 88 kHz Vycor29 sound speed data, the tunneling strength derived from the internal friction was used in the Tunneling Model fit and T_{co} was treated as a free parameter. It is encouraging to note that this

fit leads to the same deviation from the data above the peak that is well known in bulk glasses, as, for example, shown by the Suprasil W fit in Fig. 5. Slightly different values for T_{co} were derived from the variation in sound speed data as compared to the internal friction data, $T_{co}=40$ mK for the $f=88$ -kHz Vycor29 data; $T_{co}=360$ mK for the $f=20$ -MHz Vycor29 data; and $T_{co}=80$ mK for Suprasil W. Two values of γ_t are listed for both a -SiO₂ and Vycor29 in Table II, the first of which is derived from the internal friction and the second (in parentheses) from the speed of sound variation. As a demonstration of the consistency between parameters derived from the two types of experiments, the dashed line through the Vycor29 data in Fig. 4 indicates the Tunneling Model prediction for the internal friction using the T_{co} value derived from the speed of sound data. The aerogel60 data⁶⁸ included in Fig. 5 do not exhibit a maximum within the temperature range of the measurement, indicating that the maximum has been shifted to even lower temperature; the decrease in sound velocity above $T \sim 0.1$ K is characteristic of bulk amorphous solids.

The thermal conductivities of the larger porosity Vycor samples, Vycor35 and Vycor36, shown in Fig. 6, are also very similar to bulk a -SiO₂ below 0.3 K in the temperature region where phonon scattering from TLS dominates in a -SiO₂. Fits of the form $\Lambda(T) = \beta_o T^2$ [Eq. (6)] were made to the data for bulk a -SiO₂ and all Vycor samples below 0.3 K, from which the values for β_o listed in Table II were extracted. (Two values listed for Vycor29 correspond to the two differing datasets of Tait^{28,37} and Stephens²⁷ for data below 1 K.) Since the larger porosity Vycor samples were too small to perform internal friction measurements and directly extract the tunneling strength, the thermal-conductivity data in conjunction with sound speed estimates were used to estimate the tunneling strengths in Vycor35 and Vycor36. Using the β_o values from the fits and transverse sound velocities listed in Table I, tunneling strengths were derived, as listed in Table II under the heading C_Λ . The larger value of the tunneling strength derived from the thermal conductivity as compared to the internal friction for Vycor29 leads us to believe that the values of C_Λ derived for Vycor35 and Vycor36 are, if anything, overestimates.

V. DISCUSSION

Without referring to any models, some simple observations may be made. The internal friction, sound speed variation, and thermal conductivity of porous Vycor and bulk a -SiO₂ are nearly identical at low temperatures. Equally remarkable, similar statements may be made for aerogel samples with porosities as large as 88%: The magnitude of the internal friction of the aerogel samples is the same as for bulk a -SiO₂ to within a factor of 2; the thermal conductivity approaches that of a -SiO₂ at the lowest temperatures; and the variation in sound speed is similar in the aerogels and bulk a -SiO₂.

A Tunneling Model analysis of the thermal-conductivity and internal friction data indicates that the tunneling strengths $C = \bar{P} \gamma^2 / \rho v^2$ of the porous materials are well within the range typically found for bulk amorphous solids,

TABLE II. Results of Tunneling Model fits to internal friction, variation in sound speed, and thermal-conductivity data. The subscripts on $C = \bar{P}\gamma^2/\rho v^2$ refer to values determined from internal friction Q^{-1} , variation in sound speed ($\delta v/v$) and thermal-conductivity (Λ) measurements. β_o is the prefactor in the expression for the T^2 thermal conductivity [Eq. (6)]; γ_t is the coupling of TLS to transverse phonons; \bar{P} is the spectral density of TLS; and ρ is the mass density. Of the two values listed in the column for γ_t , the first is derived from Q^{-1} data and the second from $\delta v/v$ data (value in parentheses). See Table I for information on sample nomenclature.

Material	$C_{Q^{-1}}$ (10^{-4})	$C_{\delta v/v}$ (10^{-4})	C_{Λ} (10^{-4})	β_o ($10^{-4} \text{ W cm}^{-1} \text{ K}^3$)	γ_t (eV)	\bar{P} ($10^{44} \text{ J}^{-1} \text{ m}^{-3}$)	\bar{P} ($10^{38} \text{ J}^{\bar{P}^1} \text{ g}^{-1}$)
<i>a</i> -SiO ₂	3.1 ^a	3.1 ^a	3.0 ^b	3.0	0.9 (1.1) ^c	4.7 ^d	2.2 ^d
Vycor4 ^e		3.0					
Sol-gel19 ^f			5				
Vycor29 ^g	5.5		6.0, 9.0 ^h	1.73, 2.58 ^h	0.51 (0.65)	6.0 ⁱ	3.8 ⁱ
Vycor29 ^j		2.3			(0.37)		
Vycor35			8.7	1.86			
Vycor36			10	1.63			
Aerogel60 ^k	3.0	2.8					
Aerogel88 ^k	4.9	3.9					

^aReference 67. The tunneling strength derived from the $\delta v/v$ data was obtained from a fit below the low-temperature peak in $\delta v/v$, where the best agreement is typically found between values derived from Q^{-1} and $\delta v/v$ data; see Ref. 59.

^bReferences 66 and 69.

^cReference 66.

^dDetermined from a fit to the Q^{-1} data; see Eqs. (7) and (8).

^eReference 41.

^fReference 30.

^gMaterial measured in this study: Corning Code 7930.

^hSince the two thermal-conductivity datasets for Vycor29 below 1 K do not agree in the region of overlap, a value corresponding to each dataset is listed.

ⁱDetermined from a fit to the Q^{-1} data using $T_{co}=47$ mK; see Eqs. (7) and (8).

^jListed values are from our Tunneling Model fits to data from Ref. 41.

^kReferences 34 and 68. The tunneling strengths derived from the aerogel $\delta v/v$ data were obtained from fits above the low temperature peak in $\delta v/v$ where the slope is typically larger than predicted by the Tunneling Model (see Fig. 5). Consequently, the actual tunneling strengths are most likely smaller than the values listed under $C_{\delta v/v}$ for the aerogels.

as shown in Fig. 7. The pairs of horizontal lines in the figure indicate the range of tunneling strengths and elastic moduli for 47 bulk amorphous solids,⁶⁹ determined from the excitation of transverse (pair of solid lines) and longitudinal (dashed lines) phonons. For all bulk amorphous solids measured to date, the tunneling strengths are grouped within the range $5 \times 10^{-4} \leq C \leq 10^{-3}$, indicating that the tunneling strength is insensitive to chemical composition and bonding. By solely changing the *porosity* of one glass, the porous silica data shown in Fig. 7 span (and for one sample, even exceed) the entire range of elastic moduli previously covered by varying the *chemical composition* of amorphous solids, yet the tunneling strengths still fall within the same universal range.

The internal friction and speed of sound data for Vycor29 also allow us to extract the coupling constant γ and the spectral density \bar{P} along with the same quantity expressed per unit mass, \bar{P}/ρ , which is a more relevant quantity for a porous material in which a significant fraction of the volume is

occupied by voids. The spectral density per unit mass is similar in Vycor29 and bulk *a*-SiO₂ (see Table II).

Considered together, data on bulk and porous amorphous solids reveal the central result of this study—that the tunneling strength is not only independent of variations in the composition and chemical bonding of materials but is independent of their microscopic structure as well. Studies of the porous silicas show that the tunneling strength is insensitive to the porosity and microscopic structure of a material with fixed chemical composition, even under circumstances when 88% of the bulk material has been removed. Since removal of the majority of a bulk material should affect interactions, if they exist, we conclude that we find no evidence of interactions from the porous silica data.

A second conclusion can be drawn from the studies on the porous silicas: The coupling constant γ appears to scale with sound speed. This can be seen from the fact that the tunneling strength $C = \bar{P}\gamma^2/\rho v^2$ is essentially constant for the porous silicas. For Vycor29, the quantity \bar{P}/ρ is approximately

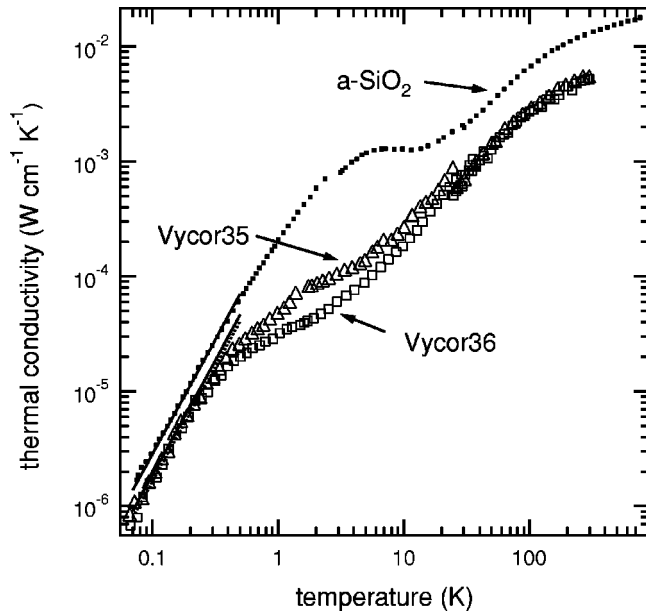


FIG. 6. Thermal conductivity of high porosity Vycor samples (this work) compared to bulk $a\text{-SiO}_2$ (Ref. 66). The thermal conductivities of $a\text{-SiO}_2$ and the Vycor samples are the same to within a factor of 2 in the temperature region below 0.3 K where scattering of phonons by TLS dominates. Lines indicate T^2 fits to the data, with prefactors listed in Table II.

the same as for bulk $a\text{-SiO}_2$; for the remaining porous silicas we assume that \bar{P}/ρ is independent of porosity (if strain-mediated interactions between TLS are responsible for the magnitude of the spectral density, \bar{P}/ρ would be expected to either remain constant or to *increase* in porous materials where a fraction of the material has been removed, allowing the TLS to become more mobile). Since $C = \bar{P}\gamma^2/\rho v^2$ and \bar{P}/ρ are essentially independent of porosity, and the speed of sound decreases with increasing porosity, the coupling between TLS and phonons, γ , must also decrease with increasing porosity. In other words, the coupling constant and the speed of sound scale with each other. The scaling is reasonable: materials with larger speeds of sound—i.e., stiffer materials—have stronger intermolecular coupling. Since the TLS are most likely groups of atoms or molecules, stronger intermolecular coupling implies stronger TLS-phonon coupling as well. The scaling is also consistent with what has been seen in bulk amorphous solids. Berret and Meissner⁷ have found that for a sampling of 18 bulk amorphous solids, γ^2 is proportional to the elastic modulus. In Fig. 8 we plot a few representative data points considered by Berret and Meissner (solid circles: transverse phonons; solid triangles: longitudinal phonons) along with our data for Vycor29 (*, 88 kHz) and our predictions for the longitudinal coupling constants in the aerogels (open triangles) [for the aerogel predictions, we use values for bulk $a\text{-SiO}_2$, $\bar{P}/\rho = 2.2 \times 10^{38} \text{ J}^{-1} \text{ g}^{-1}$ (see Table II) and $\gamma_l = 1.04 \text{ eV}$ (see Ref. 7)]. The coupling constant estimates are $\gamma_l = 0.33 \text{ eV}$ for aerogel60; $\gamma_l = 0.14 \text{ eV}$ for aerogel84; and $\gamma_l = 0.076 \text{ eV}$ for aerogel88. It would be interesting to perform low-

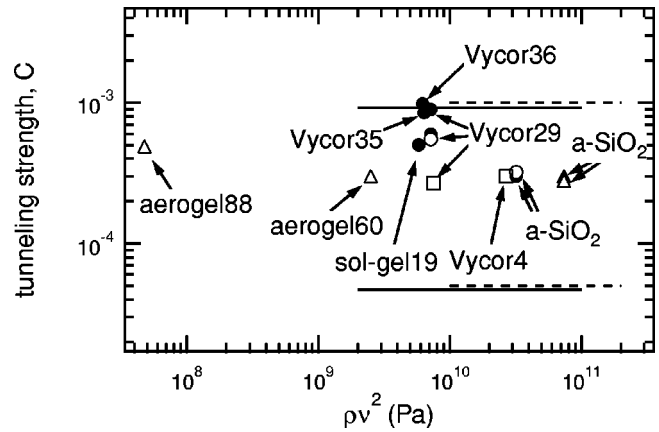


FIG. 7. A comparison of the tunneling strength $C = \bar{P}\gamma^2/\rho v^2$ of bulk $a\text{-SiO}_2$ and porous silica samples. The figure includes data extracted from internal friction measurements (measured in torsion for $a\text{-SiO}_2$ (Ref. 64) and Vycor29, open circles; and in flexure for the aerogels (Ref. 68) and $a\text{-SiO}_2$, (Refs. 69 and 65), open triangles) and from thermal-conductivity measurements for Vycor35, Vycor36, sol-gel19 (Ref. 30), and $a\text{-SiO}_2$ [Refs. 66 and 69 (solid circles)]. Also included is the tunneling strength of $a\text{-SiO}_2$ (Ref. 69) derived from the excitation of longitudinal waves (solid triangle) and the tunneling strengths for two Vycor samples (Ref. 41) (open squares; see also Table II) derived from the relative changes in sound speed data fit below the $\delta v/v$ peak. All values fall within the range spanned by the majority of bulk amorphous solids measured to date (Ref. 69), indicated by the pairs of horizontal lines for tunneling strengths derived from the excitation of transverse (solid lines) and longitudinal (dashed lines) phonons (the lines have been slightly offset for clarity). The striking observation is that materials with elastic moduli spanning three orders of magnitude have nearly identical tunneling strengths.

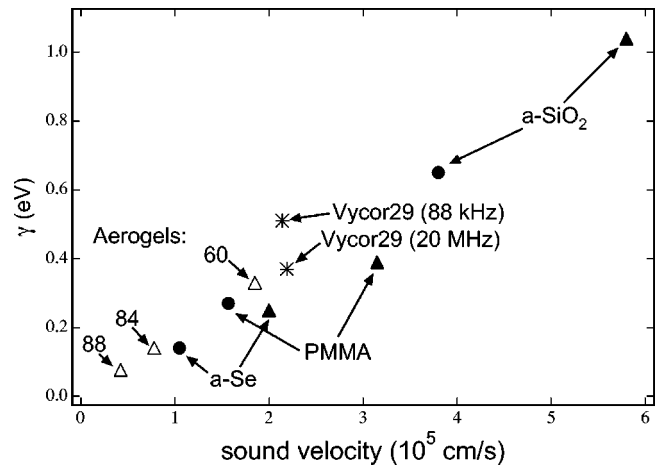


FIG. 8. Coupling constant γ between TLS and phonons as a function of sound speed for the excitation of longitudinal (\blacktriangle , \triangle) and transverse (\bullet , $*$) phonon modes. Representative data for bulk samples, from Ref. 7, indicate that the coupling constant tends to increase with increasing sound speed. Here we include data for porous Vycor29 (*; 20-MHz value is from our fit to data in Ref. 41) and predictions for the aerogel samples (\triangle) based upon our conclusion that \bar{P}/ρ is independent of porosity (see text).

temperature internal friction measurements of the aerogels to determine the coupling constants in those materials and to clarify the relation between sound speed and TLS-phonon coupling.

VI. SUMMARY

Despite significant alterations to their microscopic structure, leading to changes in the elastic modulus spanning roughly a factor 10^3 , extremely porous materials such as Vycor, sol-gel, and aerogel have TLS that behave amazingly like those in bulk amorphous solids. Internal friction, sound speed, and thermal-conductivity data indicate that the tunneling strengths of the porous materials are within the universal range found for all bulk amorphous solids, indicating that the tunneling strength is insensitive to alterations of the microscopic structure for materials of fixed chemical composition. The internal friction, sound speed, and thermal-conductivity data for the porous silicas show no evidence of interactions between TLS. The specific heats of the porous materials are significantly enhanced compared to bulk α -SiO₂, most likely

due to surface states that are weakly coupled to phonons. In addition, thermal and elastic measurements on porous silicas force upon us a conclusion not presently addressed by the theory: the coupling between TLS and phonons appears to scale with sound speed.

ACKNOWLEDGMENTS

The authors would like to thank H. J. Maris for supplying the Vycor35 and Vycor36 samples and R. D. Merithew for his help with the figures and with fits to the speed of sound data. This work was supported by the Cornell Center for Materials Research (CCMR), a Materials Research Science and Engineering Center of the National Science Foundation (Grant No. DMR-0079992). The financial support by the National Science Foundation, Grant No. DMR 9115891, is gratefully acknowledged. In addition, S.W. gratefully acknowledges the institutional and financial support of Middlebury College and the National Science Foundation (Grant No. DMR-0074930) while preparing this document.

*Present address: Physics Department, Middlebury College, Middlebury, Vermont 05753.

¹P.W. Anderson, B.I. Halperin, and C.M. Varma, *Philos. Mag.* **25**, 1 (1972).

²W.A. Phillips, *J. Low Temp. Phys.* **7**, 351 (1972).

³J. Jäckle, *Z. Phys. B* **257**, 212 (1972).

⁴W.A. Phillips, *Rep. Prog. Phys.* **50**, 1657 (1987).

⁵S. Hunklinger and W. Arnold, in *Physical Acoustics*, edited by W. P. Mason and R.N. Thurston (Academic Press, New York, 1976), p. 257.

⁶S. Hunklinger and A.K. Raychaudhuri, in *Progress in Low Temperature Physics*, edited by D.F. Brewer (Elsevier Science, North-Holland, 1985), p. 265.

⁷J.F. Berret and M. Meissner, *Z. Phys. B: Condens. Matter* **70**, 65 (1988).

⁸R.C. Zeller and R.O. Pohl, *Phys. Rev. B* **4**, 2029 (1971).

⁹M.W. Klein, B. Fisher, A.C. Anderson, and P.J. Anthony, *Phys. Rev. B* **18**, 5887 (1978).

¹⁰J.J. Freeman and A.C. Anderson, *Phys. Rev. B* **34**, 5684 (1986).

¹¹S. Hunklinger, L. Piche, J.C. Lasjaunias, and K. Dransfeld, *J. Phys. C* **8**, L423 (1975).

¹²C.C. Yu and A.J. Leggett, *Comments Condens. Matter Phys.* **14**, 231 (1988).

¹³C.C. Yu, *Phys. Rev. Lett.* **63**, 1160 (1989).

¹⁴A.J. Leggett, *Physica B* **169**, 322 (1991).

¹⁵S.N. Coppersmith, *Phys. Rev. Lett.* **67**, 2315 (1991).

¹⁶A. Burin and Y. Kagan, *Sov. Phys. JETP* **109**, 299 (1996).

¹⁷A.L. Burin, D. Natelson, D.D. Osheroff, and Y. Kagan, in *Tunneling Systems in Amorphous and Crystalline Solids*, edited by P. Esquinazi (Springer, Berlin, 1998), Chap. 5.

¹⁸A. Burin and Y. Kagan, *Phys. Lett. A* **215**, 191 (1996).

¹⁹Y. Fu, *Phys. Rev. B* **40**, 10 056 (1989).

²⁰J. Joffrin and A. Levelut, *J. Phys. (Paris)* **36**, 811 (1975).

²¹D.J. Salvino, S. Rogge, B. Tigner, and D.D. Osheroff, *Phys. Rev. Lett.* **73**, 268 (1994).

²²S. Rogge, D. Natelson, and D.D. Osheroff, *Phys. Rev. Lett.* **76**, 3136 (1996).

²³H.M. Carruzzo, E.R. Grannan, and C.C. Yu, *Phys. Rev. B* **50**, 6685 (1994).

²⁴R. Konig, M. Ramos, I. Usherov-Marshak, J. Arcas-Guijarro, A. Hernando-Maneru, and P. Esquinazi, *Phys. Rev. B* **65**, 180201 (2002).

²⁵E. Gaganidze, R. Konig, P. Esquinazi, K. Zimmer, and A. Burin, *Phys. Rev. Lett.* **79**, 5038 (1997).

²⁶J.B.E. White and R.O. Pohl, *Phys. Rev. Lett.* **75**, 4437 (1995).

²⁷R.B. Stephens, Ph.D. dissertation, Cornell University, Ithaca, NY, 1974.

²⁸R. Tait, Ph.D. dissertation, Cornell University, Ithaca, NY, 1975.

²⁹T. Klitsner and R.O. Pohl, *Phys. Rev. B* **36**, 6551 (1987). Klitsner and Pohl make the plausible argument that the majority of heat is transported by phonons of frequency $\nu_{dom} = (88.6 \text{ GHz K}^{-1})T$. In order to determine the wavelength corresponding to this frequency, we use $\lambda_{dom}\nu_{dom} = v_D$, where v_D is the Debye velocity given by $v_D = [\frac{1}{3}(1/v_l)^3 + \frac{2}{3}(1/v_t)^3]^{-1/3}$; v_l and v_t refer to the longitudinal and transverse sound velocities. For the estimates of λ_{dom} for Vycor29 and aerogel60, we use $v_l \approx 1.65v_t$ [see Eq. (5)].

³⁰J.M. Grace and A.C. Anderson, *Phys. Rev. B* **33**, 7186 (1986).

³¹D.G. Cahill, R.B. Stephens, R.H. Tait, S.K. Watson, and R.O. Pohl, in *Thermal Conductivity 21*, edited by C.J. Cremers and H.A. Fine (Plenum Press, New York, 1990).

³²R.O. Pohl, in *Amorphous Solids, Low Temperature Properties: Topics in Modern Physics*, edited by W.A. Phillips (Springer, Berlin, 1981), Vol. 24, p. 27.

³³According to the Tunneling Model, the specific heat of an amorphous solid has the form $C = AT^1 + BT^3$, where the first term is due to TLS and the second term is the Debye phonon contribution. For the aerogels, the total specific heat is less than the Debye phonon contribution at intermediate temperatures, making such fits problematical. The $C = A_oT^1$ fits shown in Fig. 2 do not include the Debye contribution and are merely intended to convey the magnitudes of the specific heats. For comparison, Grace and Anderson³⁷ found after subtracting the Debye contribution to the α -SiO₂ and sol-gel specific heats that the linear

- term was a factor of 15 larger in sol-gel than in α -SiO₂.
- ³⁴A.M. de Goer, R. Calemczuk, B. Salce, J. Bon, E. Bonjour, and R. Maynard, Phys. Rev. B **40**, 8327 (1989).
- ³⁵A. Bernasconi, T. Sleator, D. Posselt, J.K. Kjems, and H.R. Ott, Phys. Rev. B **45**, 10 363 (1992).
- ³⁶A.M. de Goer, R. Calemczuk, B. Salce, R. Maynard, and Z. Zarembovitch, Europhys. Lett. **3**, 1205 (1987).
- ³⁷R.H. Tait and J.D. Reppy, Phys. Rev. B **20**, 997 (1979).
- ³⁸E. Courtens, J. Pelous, J. Phalippou, R. Vacher, and T. Woignier, Phys. Rev. Lett. **58**, 128 (1987).
- ³⁹A. Nittke, P. Esquinazi, and A. Burin, Phys. Rev. B **58**, 5374 (1998).
- ⁴⁰A. Nittke, P. Esquinazi, H.-C. Semmelhack, A. Burin, and A. Patashinskii, Eur. Phys. J. B **8**, 19 (1999).
- ⁴¹J.R. Beamish, A. Hikata, and C. Elbaum, Phys. Rev. Lett. **52**, 1790 (1984).
- ⁴²J.H.P. Watson, Phys. Rev. **148**, 223 (1966).
- ⁴³J.H.P. Watson, Phys. Rev. B **2**, 1282 (1970).
- ⁴⁴H.J. Maris (private communication).
- ⁴⁵H.J. Maris, R.H. Torii, and G.M. Seidel, Phys. Rev. B **41**, 7167 (1990).
- ⁴⁶J.K. MacKenzie, Proc. Phys. Soc. London, Sect. B **63**, 2 (1950).
- ⁴⁷W.D. Kingery, H.K. Bowen, and D.R. Uhlmann, *Introduction to Ceramics*, 2nd ed. (Wiley, New York, 1976).
- ⁴⁸J. Hessinger, J.B.E. White, and R.O. Pohl, Planet. Space Sci. **44**, 937 (1996).
- ⁴⁹J. Gross, G. Reichenauer, and J. Fricke, J. Phys. D **21**, 1447 (1988).
- ⁵⁰T. Sleator, A. Bernasconi, D. Posselt, J.K. Kjems, and H.R. Ott, Phys. Rev. Lett. **66**, 1070 (1991).
- ⁵¹E. Courtens, R. Vacher, J. Pelous, and T. Woignier, Europhys. Lett. **6**, 245 (1988).
- ⁵²R. Calemczuk, A.M. de Goer, B. Salce, R. Maynard, and A. Zarembovitch, Europhys. Lett. **3**, 1205 (1987).
- ⁵³J.L. Smith, CRREL Technical Report No. 167, Hanover, New Hampshire, 1965 (unpublished).
- ⁵⁴R.L. Coble and W.D. Kingery, J. Am. Ceram. Soc. **39**, 377 (1956).
- ⁵⁵D.G. Cahill, Rev. Sci. Instrum. **61**, 802 (1990).
- ⁵⁶S.K. Watson and R.O. Pohl, Phys. Rev. B **51**, 8086 (1995).
- ⁵⁷D.G. Cahill and J.E.V. Cleve, Rev. Sci. Instrum. **60**, 2706 (1989).
- ⁵⁸D.G. Cahill, Ph.D. dissertation, Cornell University, Ithaca, NY, 1989.
- ⁵⁹J.E. VanCleve, Ph.D. dissertation, Cornell University, Ithaca, NY, 1991.
- ⁶⁰K.A. Topp, E. Thompson, and R.O. Pohl, Phys. Rev. B **60**, 898 (1999).
- ⁶¹J.J. DeYoreo, Ph.D. dissertation, Cornell University, Ithaca, NY, 1985.
- ⁶²A. Bernasconi, T. Sleator, D. Posselt, and H.R. Ott, Physica B **165&166**, 903 (1990).
- ⁶³A.K. Raychaudhuri and S. Hunklinger, Z. Phys. B: Condens. Matter **57**, 113 (1984).
- ⁶⁴J.E.V. Cleve, A.K. Raychaudhuri, and R.O. Pohl, Z. Phys. B: Condens. Matter **93**, 479 (1994).
- ⁶⁵J. Classen, C. Enss, C. Bechinger, G. Weiss, and S. Hunklinger, Ann. Phys. (Leipzig) **3**, 315 (1994).
- ⁶⁶K.A. Topp and D.G. Cahill, Z. Phys. B: Condens. Matter **101**, 235 (1996).
- ⁶⁷E. Thompson, G. Lawes, J.M. Parpia, and R.O. Pohl, Phys. Rev. Lett. **84**, 4601 (2000).
- ⁶⁸J. Bon, E. Bonjour, R. Calemczuk, and B. Salce, J. Phys. (Paris), Colloq. **48**, C8 (1988).
- ⁶⁹R.O. Pohl, X. Liu, and E. Thompson, Rev. Mod. Phys. **74**, 991 (2002).